Characterization of denosumab treatment response in giant cell tumors of bone with dynamic contrast-enhanced MRI

Kalisvaart, G.M.; Heijden, L. van der; Cañete, A.N.; Sande, M.A.J. van de; Gelderblom, H.; Langevelde, K. van

European Journal of Radiology 167 (2023) 111070

Contents lists available at ScienceDirect

European Journal of Radiology

journal homepage: www.elsevier.com/locate/ejrad

Characterization of denosumab treatment response in giant cell tumors of bone with dynamic contrast-enhanced MRI

G.M. Kalisvaart [a,*], L. van der Heijden [b], A. Navas Cañete [a], M.A.J. van de Sande [b,c], H. Gelderblom [d], K. van Langevelde [a]

[a] Department of Radiology, Leiden University Medical Center, Albinusdreef 2, 2333 ZA Leiden, the Netherlands
[b] Department of Orthopedics, Princess Maxima Center for Pediatric Oncology, Heidelberglaan 25, 3584 CS Utrecht, the Netherlands
[c] Department of Orthopedics, Leiden University Medical Center, Albinusdreef 2, 2333 ZA Leiden, the Netherlands
[d] Department of Medical Oncology, Leiden University Medical Center, Albinusdreef 2, 2333 ZA Leiden, the Netherlands

ARTICLE INFO

Keywords:
Giant cell tumor of bone
Magnetic resonance imaging
Denosumab
Drug monitoring
Dynamic contrast-enhanced

ABSTRACT

Rationale and objectives: Denosumab is a monoclonal antibody used neo-adjuvantly in giant cell tumor of bone (GCTB) to facilitate surgery, or long term for axial tumors where surgery comes with high morbidity. Time intervals for treatment effects to occur are unclear and monitoring tools are limited, complicating optimal drug dose titration. We assessed changes in time intensity curve (TIC) - derived perfusion features on DCE-MRI in GCTB during denosumab treatment and evaluated the duration of treatment effects on tumor perfusion.

Materials and methods: Patients with GCTB who underwent dynamic contrast enhanced (DCE) MRI before (t = 0) and after 3 (t = 3), 6 (t = 6) or 12 (t = 12) months of denosumab treatment were retrospectively included in a single center. Regions of interest were placed on tumor compartments with visually most intense enhancement and TICs were created. Time-to-enhancement (TTE), wash-in rate (WIR), maximal relative enhancement (MRE), and area-under-the-curve (AUC) were calculated. Differences in perfusion features were calculated with the Wilcoxon signed-rank test.

Results: In all 24 patients decreased perfusion on DCE-MRI after start of denosumab treatment was seen. TTE increased between t = 0 and t = 3 ($p < 0.001$). WIR, MRE and AUC decreased between t = 0 and t = 3 ($p < 0.001$, $p = 0.01$ and $p = 0.02$, respectively). No significant differences in features were found between t = 3 and t = 6 or t = 6 and t = 12. No significant perfusion differences in primary versus recurrent, or axial versus appendicular tumors, were found.

Conclusion: MRI perfusion significantly changed in GCTB within 3 months of denosumab treatment compared to baseline. No further significant change occurred between 3 and 6, and 6 and 12 months of treatment. These findings suggest that evaluation of treatment response and subsequent consideration of maintenance with lower doses of denosumab, may already be indicated after 3 months. In cases where long term denosumab is the preferred therapy, monitoring change in tumor characteristics on DCE-MRI may aid optimal drug dose titration, minimizing side effects.

1. Introduction

Giant cell tumors of bone (GCTB) are osteolytic tumors extending into the epiphysis up to the subchondral bone plate, mostly occurring around the knee, in the wrist, and in up to a third of cases in the axial skeleton. The World Health Organization (WHO) classification of soft tissue and bone tumors 2020 classifies GCTB as intermediate grade tumors as they behave locally aggressive and may metastasize to the lungs [1]. GCTB contain neoplastic mononuclear stroma cells, macrophages and abundant osteoclast-like giant cells. Denosumab is a monoclonal antibody and receptor activator of nuclear factor kappa-B (RANK)-ligand inhibitor, that functions to counteract bone resorption. It can be used in GCTB as a short neoadjuvant course, to facilitate curettage or resection by better delineation of the tumor [2]. In tumor

Abbreviations: AUC, Area-under-the-curve; DCE-MRI, Dynamic contrast-enhanced (DCE) MRI; GCTB, Giant cell tumor of bone; MRE, Maximum relative enhancement; TIC, Time intensity curves; TTE, Time-to-enhancement; WIR, Wash-in rate; RANK, receptor activator of nuclear factor kappa-B.

* Corresponding author.
E-mail address: g.m.kalisvaart@lumc.nl (G.M. Kalisvaart).

https://doi.org/10.1016/j.ejrad.2023.111070
Received 2 August 2023; Received in revised form 23 August 2023; Accepted 28 August 2023
Available online 29 August 2023

localizations where surgery would cause more morbidity than acceptable in this intermediate grade entity in young patients, such as the sacrum or (cervical) spine, long term denosumab as definitive treatment is an option.

During denosumab treatment, neo-cortex is formed and if a soft tissue component is present, it decreases in size and becomes better delineated. Within the tumor, new fibro-osseous matrix is formed and tumor density increases, which is measurable on radiographs and CT [3–5]. MRI is the modality of choice in GCTB to assess anatomical relations to surrounding structures, and also for therapy response assessment, often combined with unenhanced CT. Previous studies showed changes occurring on conventional MRI sequences (e.g. decreased signal intensity on T2 and T1 weighted sequences, and decreased cystic components in the tumor) [4].

Dynamic contrast-enhanced (DCE)-MRI has been found useful to aid in characterization of bone and soft tissue tumors [6]. GCTB show fast enhancement followed by rapid wash-out of gadolinium due to high vascularization and the small interstitial space in the tumor, a so called type IV curve [6–8]. This characteristic feature is useful in differentiation of local recurrence from postoperative granulation tissue [4]. Moreover, a recent proof-of-concept study showed that changes in perfusion characteristics on DCE-MRI at 6 months follow-up are associated with denosumab treatment induced histopathological changes in four patients [9]. In the current descriptive study we aim to assess changes in perfusion in GCTB in a larger cohort and at several timepoints during denosumab treatment, through visual assessment of time intensity curves (TIC) and comparison of TIC-derived perfusion features. In this manner, we might be able to identify the time interval where perfusion effects occur as an effect of denosumab treatment. This might be integrated in the decision making process on neoadjuvant and surgical treatment and timing of imaging for treatment monitoring in the future. Furthermore, in axial tumor cases where surgery is not feasible and long term denosumab is the preferred therapy, MRI perfusion may aid optimal drug dose titration and dose intervals, thereby preventing or minimizing side effects. Secondary aim is therefore to assess differences in perfusion characteristics between axial versus appendicular and primary versus recurrent tumors.

2. Methods

2.1. Study cohort

Patients with GCTB who were treated with denosumab at our center between 2009 and 2022 were retrospectively identified. Out of 65 initially eligible patients, 36 were excluded because DCE-MRI scans were not acquired both before and during denosumab treatment. Other exclusion criteria were DCE-MRI that were not performed in our center (n = 4) and response imaging where no lesions could be identified (n = 1). This resulted in 24 patients that were included for analyses. Complete data consisted of demographic factors, tumor characteristics, dynamic MRI before and during denosumab treatment, and histopathological evaluation of preoperative biopsy and resected/curetted tissue if available. Ethical approval was given by the local ethical committee (P12.024) and informed consent was waived.

2.2. Dynamic contrast-enhanced MRI

After conventional non-contrast imaging, tumor volume was assessed and the entire tumor volume was imaged with DCE imaging. All patients were examined with a standard imaging protocol on a 1.5 T or 3 T MRI scanner (models Intera and Ingenia, Philips Medical Systems). DCE-MRI data acquisition was started 6 s before intravenous injection of 0.2 ml/kg gadolinium contrast medium (0.5 mmol/ml) with 2 ml/s by an automatic injector. Temporal resolution ranged from 1 to 2 s during the first minute and ranged from 3 to 4 s from minute 2 to 5. Subtraction images of the DCE-MRI sequence in which the first image is subtracted from all subsequent images were generated automatically to allow construction of TICs. Baseline scans were labelled t = 0 (n = 24). Evaluation scans performed between 1.5 and 4.5 months after start of denosumab treatment were labelled t = 3 (n = 18), scans performed between 4.5 and 7.5 months after start of treatment were labelled t = 6 (n = 15), and scans performed between 10.5 and 13.5 months after start of treatment were labelled t = 12 (n = 10), representing follow-up after 3, 6 and 12 months, respectively.

2.3. Imaging assessment

All DCE-MRI images were processed in Philips IntelliSpace Portal (version 12, Philips Medical Systems) and segmented by a dedicated musculoskeletal oncology radiologist (5 years of experience). After visual evaluation of the whole tumor volume on DCE-MRI, a circular region of interest (ROI) was placed on the closest regional artery and 3 circular ROIs of 20–40 mm^2 were placed on separate tumor compartments with most intense enhancement. This segmentation method was selected to provide an easily applicable and practical method accounting for tumor heterogeneity without resulting measurements being effected by cystic components typically seen in GCTB. Signal intensities of the 3 tumor ROIs were averaged to globally represent tumor enhancement and improve repeatability. Intensity curves were created for the artery and tumor ROIs. Four TIC-derived perfusion characteristics, being time-to-enhancement (TTE), wash-in rate (WIR), maximal relative enhancement (MRE), and area-under-the-curve, were calculated and studied according to methods used in earlier work (Fig. 1) [10]. Differences in features between axial versus appendicular, primary versus recurrent GCTB and features before and after treatment were tested for significance with the Wilcoxon signed-rank test. P-values < 0.05 were considered statistically significant. Relative change in perfusion features was calculated by dividing features on response scans by features on baseline scans. For visual assessment of TICs, all artery- and

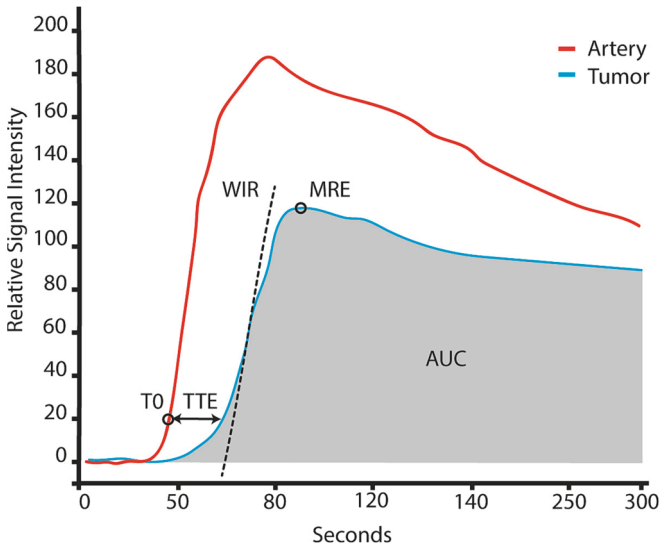

Fig. 1. Schematic dynamic contrast-enhanced MRI derived time-intensity curve and perfusion features for an artery and a tumor region depicting changes in average pixel signal intensity over time due to influx and outflux of gadolinium contrast medium. Time of onset of enhancement (T0), the first timepoint at which the artery signal intensity increases for more than 20% compared to baseline, was determined to allow calculation of time-to-enhancement (TTE) of the tumor. Wash-in rate (WIR) was defined as maximum percentual rise in signal intensity per second. Maximum relative enhancement (MRE) was defined as the signal intensity relative to baseline at point of maximum enhancement. Area-under-the-curve (AUC) was defined as the sum of all intensity relative to baseline for the first 90 s. This figure was reproduced with permission from Kalisvaart and Van Den Berghe et al. [10].

corresponding tumor TICs were translated to time of first 20% intensity increase of artery ROI is time = 0 s, allowing plotting of mean artery and tumor TICs and construction of 95% confidence intervals (95%CI) for signal intensities per time-point. All 95%CIs presented in this study are calculated as $\mu \pm 1.96*\sigma/\sqrt{n}$, where μ is the mean intensity at a time-point, σ is the standard deviation and n is the number of cases included.

3. Results

3.1. Population and treatment characteristics

Complete data sets were available for 24 patients treated with denosumab and median age was 37 years (range 18–60) (Table 1). Fifteen patients received denosumab for GCTB in the appendicular skeleton and nine for GCTB in the axial skeleton. Thirteen patients received denosumab for primary GCTB and 11 patients for recurrent GCTB after previous surgical treatment. Median days between baseline (t = 0) DCE-MRIs and start of denosumab treatment was 32 days (range = 0–113, n = 24). Complications of denosumab included osteonecrosis of the jaw in one patient, for which denosumab was stopped. Complications of surgical treatment were infection in two patients, for which intravenous antibiotics were given resulting in full recovery; transient neuropraxia in one patient; and permanent T1 nerve damage in one patient (Table 2). After denosumab treatment, primary surgical treatment consisted of intralesional curettage with or without local adjuvants (n = 22), resection (n = 1) or none (n = 1). Median follow-up was 4.6 years (range 1–11). Six patients had further local recurrences, treated with curettage with or without local adjuvants (n = 3), resection (n = 2) or no surgery (n = 1).

3.2. Perfusion characteristics during treatment

Visual assessment of mean TICs showed relatively early and steep enhancement followed by slow wash-out of contrast before start of treatment at t = 0 (Fig. 2**A**). A significant delay in arrival of contrast and reduced enhancement is seen within 3 months of treatment (Fig. 3). The 95% confidence intervals of TICs at t = 3 and t = 6 overlap, although a slight increase in persisting enhancement is seen at t = 6. The mean TIC of 2 cases who underwent the earliest follow-up scans, after approximately 2 months of treatment, lies within the 95% confidence interval of follow up scans at every time point.

TTE significantly increased between t = 0 and t = 3 ($p < 0.001$), t = 6 ($p = 0.02$) and t = 12 ($p = 0.007$) (Fig. 2**B**). For WIR, significant decreases were seen between t = 0 and t = 3 ($p < 0.001$), t = 6 ($p = 0.02$) and t = 12 ($p = 0.04$). For MRE and AUC, significant decreases were also seen between t = 0 and t = 3 ($p = 0.01$ and $p = 0.02$, respectively), while no significant difference was found between t = 0 and t = 6 ($p = 0.10$ and $p = 0.07$, respectively) and t = 0 and t = 12 ($p = 0.07$ and $p = 0.09$, respectively). For all 4 features no significant change was seen between t = 3 and t = 6, and between t = 6 and t = 12 ($p > 0.5$ for all). Feature values and relative changes are reported in Table 3.

3.3. Perfusion characteristics of axial versus appendicular tumors

Mean TICs of appendicular tumors show on average quicker and faster enhancement than in axial tumors before start of treatment at t = 0, although 95% confidence intervals overlap for every time point (Fig. 4**A**).

At t = 0 no significant difference is seen between appendicular and axial tumors differences in TTE ($p = 0.88$), WIR ($p = 0.20$), MRE ($p = 0.13$), and AUC ($p = 0.13$) (Fig. 4**B**). There were 2 cases, which demonstrated < 25% reduction in WIR, MRE and AUC at t = 3, in contrast to all other cases. Both these cases had sacral GCTB localizations.

3.4. Perfusion characteristics of primary versus recurrent tumors

Primary and recurrent tumors visually have comparable TICs at baseline before treatment (Fig. 4**C**).

Also in this subgroup analysis, no significant difference is seen at t = 0 between in TTE ($p = 0.70$), WIR ($p = 0.54$), MRE ($p = 0.80$), and AUC ($p = 0.75$) (Fig. 4**D**).

Table 1
Patient, tumor, neoadjuvant treatment and imaging characteristics.

Patient	Sex	Age (years)	Localization	Soft tissue extension (y/n)	Pathologic fracture (y/n)	Primary (p) /recurrent (r)	neoadjuvant denosumab doses (n)	MRI at t = 3 (y/n)	MRI at t = 6 (y/n)	MRI at t = 12 (y/n)
1	M	52	ischium	y	n	p	8	y	y	n
2	M	42	distal tibia	y	n	r	25	y	y	y
3	M	21	distal femur	y	y	r	19	y	y	y
4	F	18	distal radius	y	n	p	13	y	y	y
5	F	40	distal ulna	y	n	p	8	y	y	y
6	M	19	sacrum	y	n	r	12	y	n	n
7	M	19	distal femur	y	n	r	13	y	y	y
8	M	43	metacarpal 3	y	n	r	11	n	y	n
9	M	37	proximal radius	y	n	p	12	n	n	y
10	M	57	distal radius	y	n	p	10	n	y	n
11	M	41	sacrum	y	n	p	12	y	y	n
12	F	57	proximal tibia	y	n	r	18	y	n	y
13	F	26	proximal tibia	y	y	p	12	n	y	n
14	F	60	proximal tibia	y	n	r	3	y	n	n
15	F	30	distal radius	y	n	p	6	y	n	n
16	F	36	proximal tibia	y	y	r	6	n	y	n
17	M	19	C5-C7	y	y	p	4	y	n	n
18	F	43	metatarsal 3	y	n	r	4	y	n	n
19	F	36	Th1	y	n	p	10, thereafter 3-monthly	y	n	y
20	F	51	C7-Th1	y	n	p	4	y	n	n
21	F	46	proximal humerus	y	n	r	5	n	y	n
22	M	59	sphenoid	y	n	p	10	y	y	n
23	M	23	sacrum	y	n	p	4	y	n	y
24	F	20	sacrum	y	n	r	15	y	y	y

M = male, F = female, y/n = yes (present) or no (not present), MRI = magnetic resonance imaging, t = 3/6/12 in months after start denosumab.

Table 2
Treatment and follow-up after denosumab treatment.

Patient	Surgery	Adjuvant denosumab doses (n)	recurrence and treatment	complication	Follow-up (months)
1	curettage, phenol, PMMA	5	–	–	48
2	resection	0	–	–	54
3	curettage, phenol, PMMA	6	–	–	39
4	curettage, phenol, PMMA	6	–	–	71
5	curettage, phenol, PMMA	0	resection	Osteonecrosis of the jaw	59
6	embolization, curettage	6	–	–	95
7	curettage, phenol, PMMA	6	–	–	53
8	curettage, phenol, PMMA	6	–	–	88
9	curettage, phenol, PMMA	0	resection	–	77
10	curettage, phenol, PMMA	6	–	infection	56
11	curettage	0	–	–	47
12	no surgery	no surgery	–	–	60
13	curettage, phenol, PMMA	6	curettage, phenol, PMMA	–	59
14	curettage, phenol, PMMA	0	–	–	77
15	curettage, phenol, PMMA	0	–	neuropraxia transient	50
16	curettage, phenol, PMMA	0	curettage, phenol, PMMA	–	142
17	resection	0	–	–	37
18	resection	0	–	–	41
19	no surgery	no surgery	–	T1 nerve damage	94
20	curettage	0	curettage	infection	72
21	cuettage, phenol, PMMA	0	resection	–	84
22	no surgery yet	no surgery yet	–	–	10
23	curettage	3 monthly	residual tumor	–	14
24	embolization, curettage	12	resection	–	29

PMMA = polymethylmethacrylate.

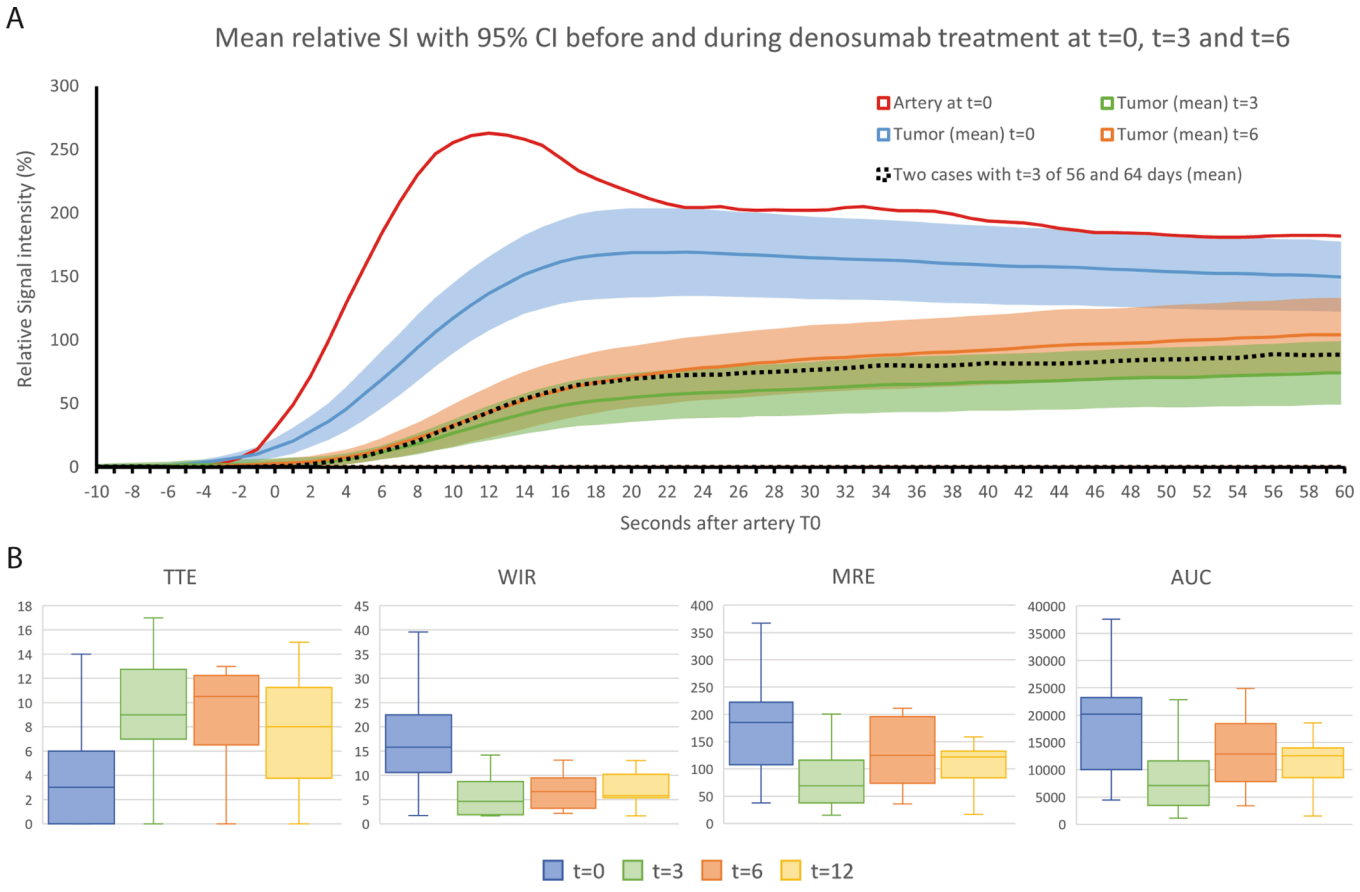

Fig. 2. **A:** Time-intensity curve for tumors at baseline (t = 0, n = 24), at 3 months after start denosumab (t = 3, n = 18) and 6 months after start denosumab (t = 6, n = 15). The mean time-intensity curve for the 2 patients with the earliest evaluation scan after start denosumab (54 and 64 days) is shown to be within the 95% confidence interval of all time-intensity curves at t = 3. **B:** Features time-to-enhancement (TTE), wash-in rate (WIR), maximum relative enhancement (MRE) and area-under-the-curve (AUC) at baseline (t = 0, n = 25), at 3 months after start denosumab (t = 3, n = 18), 6 months after start denosumab (t = 6, n = 14) and 12 months after start denosumab (t = 12, n = 10). Boxes and whiskers represent interquartile ranges (IQR) and ranges, respectively. Ranges exclude outliers, defined as values 1.5 times the IQR below the 1st quartile or 1.5 times the IQR above the 3rd quartile.

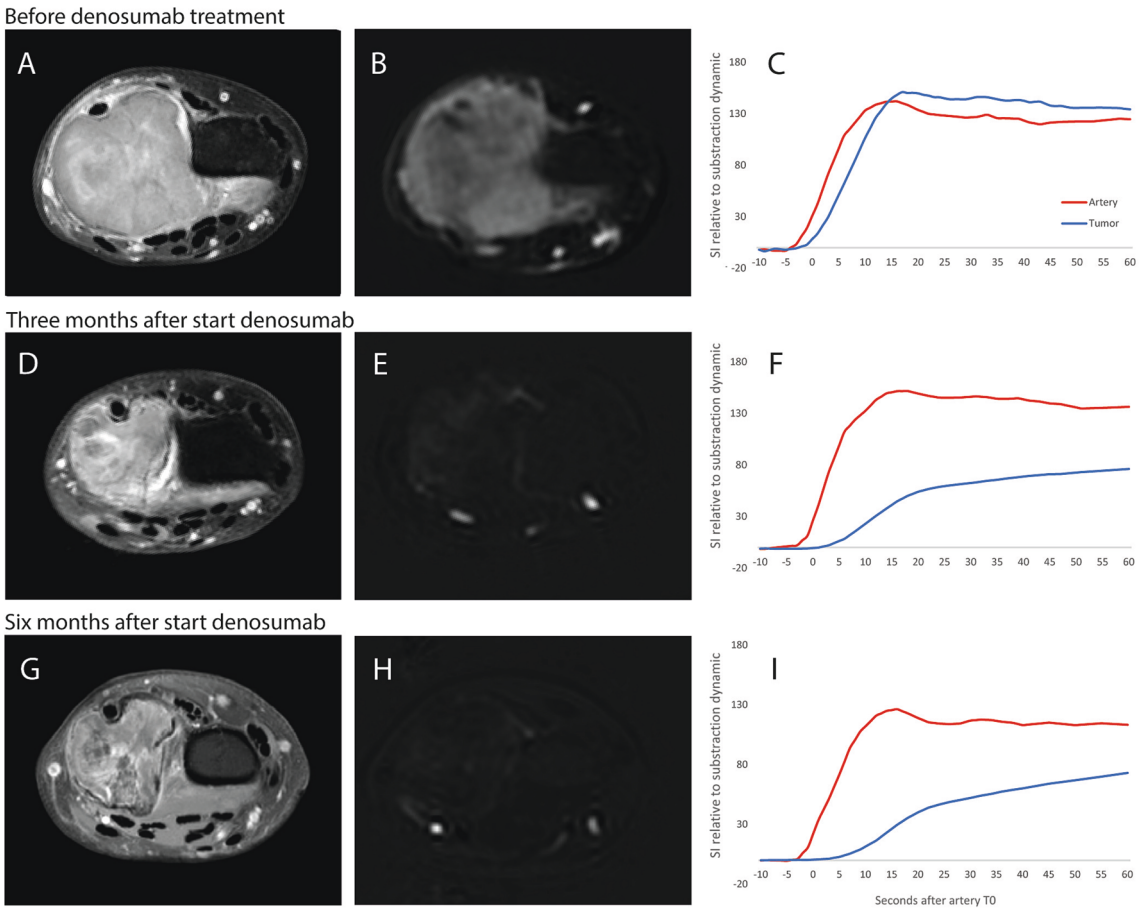

Fig. 3. GCTB of the distal ulna with representative response to denosumab on DCE-MRI. Images A-C: at baseline, before start of denosumab treatment. Images D-F: after 3 months on denosumab treatment. Images G-I after 6 months of denosumab treatment. *A, D and G: Axial T1 SPIR post contrast over time. B, E and H: Snapshot images of subtraction DCE-MRI at 10 s after contrast arrival in feeding arteries. Note the delay and reduction in tumor enhancement after denosumab treatment. C, F and I: TIC of artery and tumor at baseline, 3 months and after 6 months of start denosumab showing decreased tumor perfusion after treatment. Time-to-enhancement increased during treatment and was 1, 10 and 13 s for t = 0, t = 3 and t = 6 respectively. Wash-in rate, maximal relative enhancement and area-under-the-curve decreased in the first 3 months and changed minimally between 33 and 6 months. WIR was 12.1 s^{-}, 3.8 s^{-} and 3.3 s^{-}. MRE 151.3, 87.5 and 91.5. AUC was 22.3x10^{3}, 9.1x10^{3} and 88.8x10^{3}.*

Table 3
Median perfusion features and median changes in perfusion features with corresponding interquartile ranges.

Perfusion features per time point					
Time point	**Inclusions (n)**	**TTE (s)**	**WIR (s^{-})**	**MRE**	**AUC x10^3**
t = 0	24	3.0 (0.0–6.0)	15.8 (10.6–22.5)	185.4 (107.5–222.2)	20.2 (10.0–23.2)
t = 3	18	9.0 (7.5–13.5)	4.6 (1.9–8.7)	68.6 (37.5–116.1)	7.1 (3.4–11.6)
t = 6	15	10.5 (6.5–12.3)	6.6 (3.2–9.5)	125 (73.8–195.6)	12.9 (7.8–18.5)
t = 12	10	8.0 (4.5–11.5)	5.8 (5.3–10.2)	122 (83.7–132.9)	12.5 (8.6–14.0)
Relative change in perfusion features per follow-up scan relative to baseline					
Time point	**Inclusions (n)**	**relative TTE**	**relative WIR**	**relative MRE**	**relative AUC**
t = 3	18	2.83 (1.45–6.15)	0.30 (0.22–0.53)	0.47 (0.21–0.79)	0.43 (0.21–0.88)
t = 6	15	1.75 (1.38–6.38)	0.47 (0.24–0.72)	0.82 (0.44–1.38)	0.84 (0.43–1.33)
t = 12	10	4.00 (1.83–5.50)	0.41 (0.19–1.01)	0.73 (0.41–1.08)	0.74 (0.41–1.07)
Perfusion features for axial and appendicular tumors at baseline (t = 0)					
Location	**Inclusions (n)**	**TTE (s)**	**WIR (s^{-})**	**MRE**	**AUC x10^3**
Axial	9	3.0 (0.5–5.8)	14.2 (5.3–16.3)	123.1 (53.4–191.6)	12.6 (5.6–21.9)
Appendicular	15	3.0 (0.0–6.0)	18.4 (11.7–23.7)	197.4 (139.3–227.4)	22.1 (15.5–24.2)
Perfusion features for primary and recurrent tumors at baseline (t = 0)					
Primary/recurrent	**Inclusions (n)**	**TTE (s)**	**WIR (s^{-})**	**MRE**	**AUC x10^3**
Primary tumor	13	2.0 (0.5–5.5)	16.0 (12.6–27.2)	186.5 (123.1–224.1)	20.1 (12.3–23.6)
Recurrent tumor	11	5.0 (0.0–6.0)	16.1 (9.6–21.4)	184.2 (95.1–222.9)	18.7 (8.8–23.4)

TTE = time-to-enhancement, WIR = wash-in rate, MRE = maximal relative enhancement, AUC = area-under-the-curve.

4. Discussion

In this study we demonstrated changes in perfusion on DCE-MRI in 24 GCTB cases as a sign of denosumab treatment response. We found a significant delay in arrival of contrast and reduced enhancement at 3 months of denosumab treatment compared to baseline. No further change in TTE, WIR, MRE and AUC occurred at 6 or 12 months. We identified no non-responders in our cohort. Recurrent tumors showed

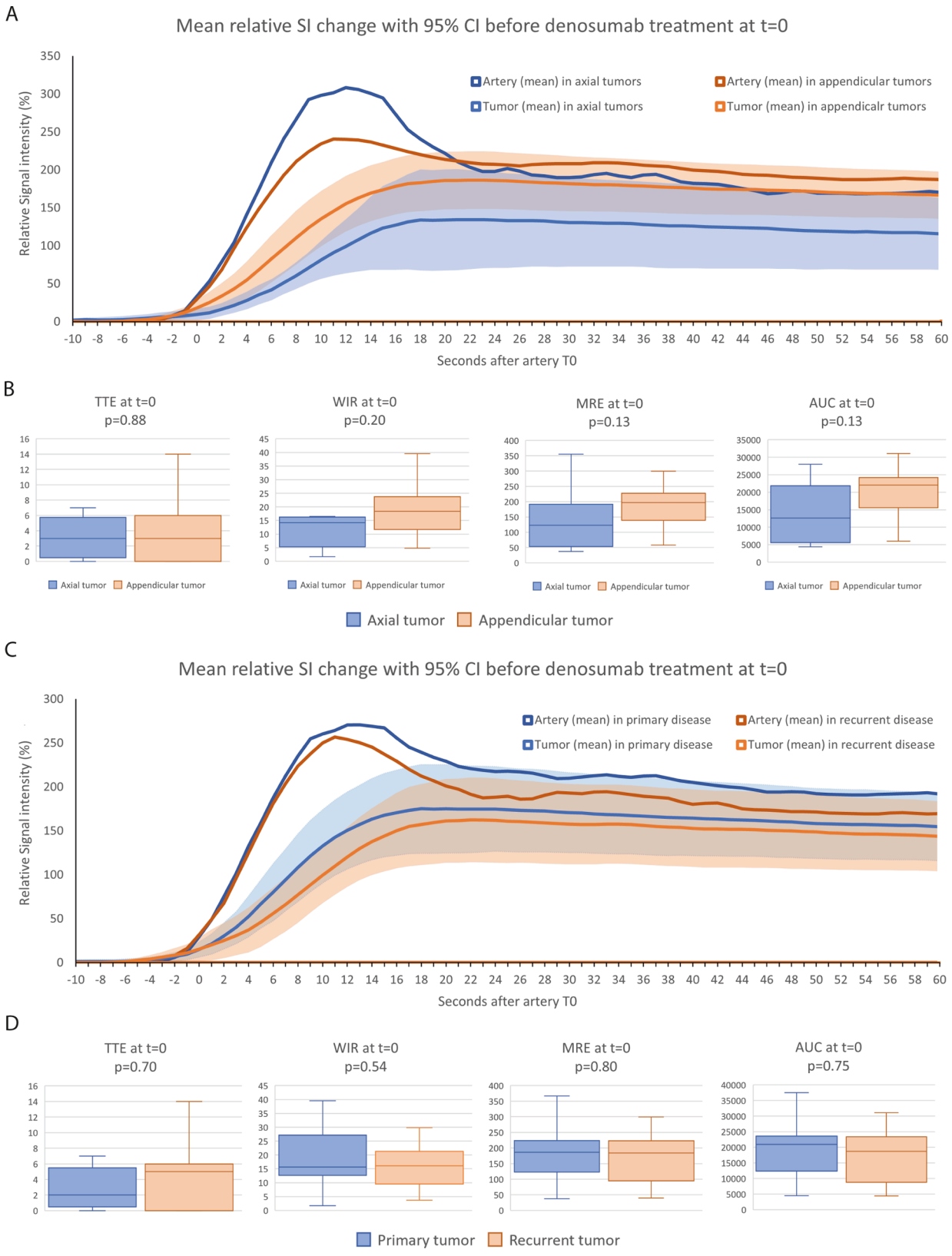

Fig. 4. **A:** Time-intensity curve for axial and appendicular tumors at baseline (t = 0, n = 9 and n = 15, respectively) and at 3 months after start denosumab (t = 3, n = 8 and n = 10, respectively). **B:** Features time-to-enhancement (TTE), wash-in rate (WIR), maximum relative enhancement (MRE) and area-under-the-curve (AUC) at baseline (t = 0) for axial (n = 9) and appendicular (n = 15) tumors. Boxes and whiskers represent interquartile ranges (IQR) and ranges, respectively. Ranges exclude outliers, defined as values 1.5 times the IQR below the 1st quartile or 1.5 times the IQR above the 3rd quartile. **C:** Time-intensity curve for primary and recurrent tumors at baseline (t = 0, n = 13 and n = 11, respectively) and at 3 months after start denosumab (t = 3, n = 10 and n = 9, respectively). **D:** Features time-to-enhancement (TTE), wash-in rate (WIR), maximum relative enhancement (MRE) and area-under-the-curve (AUC) at baseline (t = 0) for primary (n = 13) and recurrent (n = 11) tumors.

the same perfusion behavior as primary tumors. Appendicular tumors showed faster enhancement than axial tumors before starting treatment, although this was not statistically significant.

The typical type IV TIC in GCTB, i.e. fast enhancement followed by slow wash-out of contrast, is well known [4,11–12]. This is a useful radiological characteristic in differentiating tumor recurrence from postoperative changes for example, and also in differentiation between spinal chordomas from GCTB. The fast enhancement followed by wash-out in GCTB can be explained by a high micro vessel density and leaky vessels with high permeability on microscopy [12]. A proof-of-concept study by Lejoly et al. showed perfusion on DCE-MRI decreased after 6 months of treatment with denosumab in six patients [9]. Nevertheless, from previous studies we know denosumab effects can be seen as early as after 2 weeks on radiographs [13] and after 8 weeks on ([^{18}F]FDG-PET) CT [4]. To our knowledge, the current study is the first to quantify denosumab treatment effect by DCE-MRI as early as 3 months after start of treatment, and at multiple timepoints in follow-up. Our results show MRI perfusion may be beneficial for insight in treatment response in case of a short neoadjuvant presurgical approach, by monitoring perfusion effects and determining the timepoint of maximum biological therapy effects being achieved. However, especially in axial tumor localizations such as the cervical spine or sacrum, surgical treatment comes with high morbidity due to the sacrifice of nerve roots, and long term denosumab therapy may provide an alternative to morbid surgery. For these cases, monitoring of TIC during MRI follow up could be helpful and future studies may focus on optimal drug dose titration and optimal treatment intervals for chronic denosumab treatment (Fig. 5).

Average changes in WIR and AUC after 6 months of treatment were determined both in the study by Lejoly et al. and the current study. Although comparison is complicated by differences in ROI selection- and feature calculation methods, features decreased in both studies affirming robustness of results. In addition, the current study shows this decrease was already present after 3 months of treatment. These findings suggest the desired treatment effects might already be reached as early as three months after start of treatment, underlining results of recent studies showing short-course neoadjuvant denosumab (<3 months) might be as effective as longer courses of neoadjuvant denosumab [14]. Our cohort included 2 cases with sacral GCTB localizations, which demonstrated < 25% reduction in WRE, MRE and AUC after 3 months of treatment, in contrast to all other cases. In both cases imaging protocols, segmentations and pathology reports were re-evaluated, but no distinctions were found. Specifically, no malignant transformation was reported during follow-up or in the resected material. These findings may be partially explained by relatively high vascularization often seen in sacral GCTB [15,16].

This study has limitations. As all cases showed largest change in TTE, WIR, MRE and AUC between t = 0 and t = 3, it would have been interesting to have more detailed insight in the exact time course of

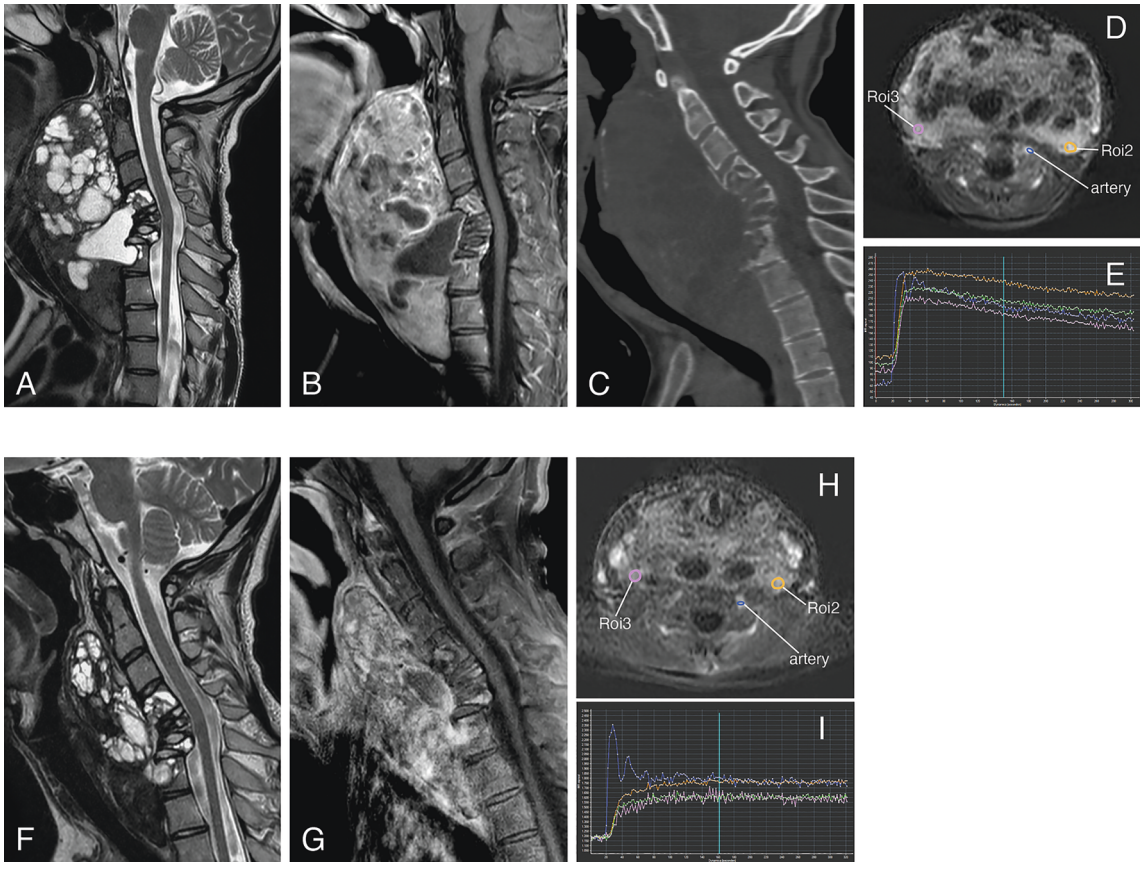

Fig. 5. GCTB of the cervical spine. Images A-E: at baseline, before start of denosumab treatment. Images F-I: after 2 months on denosumab treatment. *A: Sagittal T2-weighted MRI image shows a tumor originating from the C4-C7 vertebral bodies, accompanied by a large prevertebral soft tissue mass. The tumor caused cervical kyphosis due to collapse of C5 and C6 with retropulsion. Note the low signal in the tumor and the multiple cystic components, typical for GCTB. B: Sagittal T1 SPIR post contrast shows solid enhancement of the low T2 areas and rim enhancement of the cystic components. C: Sagittal CT image demonstrates an expansile osteolytic tumor with a thin interrupted bony shell surrounding the soft tissue mass. D: snapshot image of subtraction DCE-MRI with a ROI in the artery (blue) and two ROIs in the solid enhancing areas of the tumor (orange and purple). E: TIC at baseline demonstrated fast enhancement in 3 ROIs placed in the tumor, within 10 s after the artery followed by wash-out (type IV curve). Note that the green ROI is not shown in figure D. F: Sagittal T2-weighted MRI image shows a marked volume decrease in the soft tissue component and of the cystic areas after 2 months on denosumab treatment. G: Sagittal T1 SPIR post contrast (suboptimal image quality due to artefacts) shows persistent heterogeneous enhancement. H and I: snapshot image of subtraction DCE-MRI with a ROI in the artery (blue) and two ROIs in the solid enhancing areas of the tumor (orange and purple), the green curve ROI is not shown in figure H. TTE increased, whereas MRE, wash-out and AUC compared to the artery decreased on denosumab treatment.*

treatment effect on perfusion during the first 3 months. The mean TIC of 2 cases who underwent the earliest follow-up scans, at approximately 2 months after start treatment, was within the 95% confidence interval of follow up scans at every time point, suggesting change in perfusion already occurs within 2 months. Easily applicable regional segmentation of most aggressive tumor areas, rather than more time intensive whole tumor volume segmentation, was performed to warrant clinical practicability of used methods. Future studies might compare the value of different segmentation methods in DCE-MRI for characterization of GCTBs. Furthermore, radiographs and/or CT scans were performed at the time of diagnosis, but not regularly during follow up in this patient group. No Tofts modelling was performed on our data because T1-mapping was not available in the retrospective study. Also, no questionnaires to quantify clinical response were studied. Correlation of tumor density (in Hounsfield units), pharmacokinetic modelling of quantitative permeability features and clinical response to MRI perfusion might have additional value in future studies.

In conclusion, we found that MRI perfusion significantly changed in GCTB within 3 months of denosumab treatment. There was delay in arrival of contrast and reduced enhancement within 3 months of denosumab treatment compared to baseline. No further change in perfusion parameters occurred at $t = 6$ or $t = 12$. These findings suggest that response monitoring with DCE-MRI and subsequent deliberations on maintenance treatment with lower dose and increased intervals may already be considered as early as after three months, potentially reducing denosumab related toxicity in a young patient population. In axial tumor cases where surgery is not feasible and long term denosumab is the preferred therapy, MRI perfusion may aid optimal drug dose titration and dose intervals, thereby preventing or minimizing side effects.

5. Declaration of Generative AI and AI-assisted technologies in the writing process

During the preparation of this work the author(s) did not use generative AI and AI-assisted technologies.

CRediT authorship contribution statement

G.M. Kalisvaart: Methodology, Formal analysis, Writing – original draft, Visualization. **L. van der Heijden:** Data curation, Writing – original draft, Writing – review & editing, Methodology, Investigation. **A. Navas Cañete:** Resources, Writing – review & editing, Methodology, Investigation. **M.A.J. van de Sande:** Conceptualization, Resources, Writing – review & editing, Methodology, Investigation, Supervision. **H. Gelderblom:** Conceptualization, Resources, Writing – review & editing, Methodology, Investigation, Supervision. **K. van Langevelde:** Conceptualization, Data curation, Writing – original draft, Writing – review & editing, Methodology, Investigation, Supervision.

Declaration of Competing Interest

The authors declare that they have no known competing financial interests or personal relationships that could have appeared to influence the work reported in this paper.

References

[1] WHO Classification of Tumours. Soft Tissue and bone tumours. 5 ed. Lyon, France: International Agency for Research on Cancer; 2020.
[2] L. van der Heijden, A. Lipplaa, K. van Langevelde, J. Bovée, M.A.J. van de Sande, H. Gelderblom, Updated concepts in treatment of giant cell tumor of bone, Curr. Opin. Oncol. 34 (4) (2022) 371–378.
[3] Y.C. Chang, R. Stoyanova, S. Danilova, et al., Radiomics on radiography predicts giant cell tumor histologic response to denosumab, Skeletal Radiol. 50 (9) (2021) 1881–1887.
[4] K. van Langevelde, C.L. McCarthy, Radiological findings of denosumab treatment for giant cell tumours of bone, Skeletal Radiol. 49 (9) (2020) 1345–1358.
[5] J. Engellau, L. Seeger, R. Grimer, et al., Assessment of denosumab treatment effects and imaging response in patients with giant cell tumor of bone, World J. Surg. Oncol. 16 (1) (2018) 191.
[6] J.L. Drapé, Advances in magnetic resonance imaging of musculoskeletal tumours, Orthopaed. Traumatol., Surg. Res.: OTSR 99 (1 Suppl) (2013). S115-23.
[7] K.L. Verstraete, H.J. Van der Woude, P.C. Hogendoorn, Y. De-Deene, M. Kunnen, J. L. Bloem, Dynamic contrast-enhanced MR imaging of musculoskeletal tumors: basic principles and clinical applications, J. Magn. Reson. Imaging 6 (2) (1996) 311–321.
[8] L. Chen, X.Y. Ding, C.S. Wang, M.J. Si, L.J. Du, Y. Lu, Triple-phase dynamic MRI: a new clue to predict malignant transformation of giant cell tumor of bone, Eur. J. Radiol. 83 (2) (2014) 354–359.
[9] M. Lejoly, T. Van Den Berghe, D. Creytens, et al., Diagnosis and monitoring denosumab therapy of giant cell tumors of bone: radiologic-pathologic correlation, Skeletal Radiol. (2023).
[10] G.M. Kalisvaart, T. Van Den Berghe, W. Grootjans, et al., Evaluation of response to neoadjuvant chemotherapy in osteosarcoma using dynamic contrast-enhanced MRI: development and external validation of a model, Skeletal Radiol. (2023).
[11] M. Libicher, L. Bernd, J.P. Schenk, U. Mädler, L. Grenacher, G.W. Kauffmann, Characteristic perfusion pattern of osseous giant cell tumor in dynamic contrast-enhanced MRI, Der Radiologe 41 (7) (2001) 577–582.
[12] N. Lang, M.Y. Su, X. Xing, H.J. Yu, H. Yuan, Morphological and dynamic contrast enhanced MR imaging features for the differentiation of chordoma and giant cell tumors in the Axial Skeleton, J. Magn. Reson. Imaging 45 (4) (2017) 1068–1075.
[13] D. von Borstel, A.R. Taguibao, A.N. Strle, E.J. Burns, Giant cell tumor of the bone: aggressive case initially treated with denosumab and intralesional surgery, Skeletal Radiol. 46 (4) (2017) 571–578.
[14] S. Hindiskere, C. Errani, S. Doddarangappa, V. Ramaswamy, M. Rai, P.S. Chinder, Is a Short-course of Preoperative Denosumab as Effective as Prolonged Therapy for Giant Cell Tumor of Bone? Clin. Orthop. Relat. Res. 478 (11) (2020) 2522–2533.
[15] P.P. Lin, V.B. Guzel, M.F. Moura, et al., Long-term follow-up of patients with giant cell tumor of the sacrum treated with selective arterial embolization, Cancer 95 (6) (2002) 1317–1325.
[16] S.-H. He, W. Xu, Z.-W. Sun, et al., Selective Arterial Embolization for the Treatment of Sacral and Pelvic Giant Cell Tumor: A Systematic Review, Orthop. Surg. 9 (2) (2017) 139–144.